Proceedings of ASME Turbo Expo 2011
GT2011
June 6-10, 2011, Vancouver, British Columbia, Canada

GT2011-45705

HOT-ACOUSTIC-TESTRIG (HAT) - A UNIQUE FACILITY FOR THERMOACOUSTIC RESEARCH

Karsten Knobloch, Claus Lahiri, Lars Enghardt, and Friedrich Bake
German Aerospace Center (DLR)
Institute of Propulsion Technology
D-10623 Berlin, Germany
Email: karsten.knobloch@dlr.de

Dieter Peitsch
Department of Aeronautics and Astronautics
Berlin Institute of Technology
D-10587 Berlin, Germany

ABSTRACT

A modular test facility for the investigation of thermoacoustic phenomena has been constructed in Berlin, which exhibits the accuracy of laboratory experiments with well defined boundary conditions. Moreover, the facility provides independent control of temperature, operating pressure and flow velocity up to a range relevant for real gas turbine applications. The unique facility is decribed in detail with an emphasis on instrumentation to be used for acoustic investigations and the data assessment procedure for the investigation of bias flow liner damping characteristics as the primary reasearch target for the initial operation. An outlook is given with respect to options und upgrades planned for the future.

NOMENCLATURE

M mean grazing flow Mach number
R energy reflection coefficient
T energy transmission coefficient
c speed of sound
k wave number
$\hat{p}$ complex sound pressure
r reflection coefficient, duct radius
t transmission coefficient, liner thickness
$\tilde{u}$ jet velocity of zero-mass-flow liner
x axial coordinate
Δ energy dissipation coefficient
ρ density
ω angular fequency
a,b subscripts referring to measurements A and B
$1,2$ subscripts referring to sections 1 and 2
$+,-$ superscripts referring to the downstream and upstream directions

INTRODUCTION

The understanding of thermoacoustic phenomena is crucial for reducing pollutant and noise emissions and increasing the efficiency of modern gas turbines. Performing combustion tests is very complex and oftentimes only provides a limited insight into the many individual physical mechanisms. On the other hand, test facilities operating at isothermal and atmospheric conditions are able to deliver results of high accuracy, however neglecting the effects of the high temperature and high pressure. The new Hot-Acoustic-Testrig (HAT) fills this gap and is able to maintain a high accuracy at almost realistic engine conditions. In its current setup the HAT allows high accuracy measurements of the acoustic properties of perforated liners. Unlike a combustion rig the air is heated by an electric heater and the acoustic excitation is provided by loudspeakers, hence, allowing the independent control of the thermodynamic properties and the acoustic excitation.

The DLR department of Engine Acoustics has a strong background in the investigation of liners. This includes for example so called Helmholtz-liners which are subjected to a grazing flow

and provide high acoustic damping, but only within a small bandwith. A second type of liners are perforated liners which are usually combined with a bias flow going through the perforation. These liners are used to suppress thermoacoustic instabalities by the effective dissipation of acoustic energy. Both types of liners have been studied very carefully by measuring transmission, reflection and dissipation of acoustic energy in a dedicated facility, the DUCT facility at DLR Berlin (see e.g. [1], [2]). This test facility can accept both liner types in either a circular or rectangular test section and operates at ambient conditions. The grazing flow is limited to Ma=0.27 and the upper frequency limit is given by the cut-on frequency of the first higher order mode (about 1400 Hz for the circular, and 2300 Hz for the rectangular test section).

Although this facility provides results of excellent accuracy (dissipation error below 1 % for most of the frequency range), a distinct uncertainty is connected with the extrapolation of these results to the actual liners to be applied to aero engines. Therefore, the erection of a new facility was planned, which increases the Mach number and frequency range which can be investigated and includes the effects of elevated pressure and temperature at the same time. The modular construction of the facility allows easy and cost-effective adaptations for various investigations as will be highlighted in the outlook. The commissioning is planned for December 2010 with many projects for bias-flow liners already scheduled.

EXPERIMENTAL SETUP

The general setup and working principle follows closely the design of the DUCT facility, which has been extensively used for investigations at ambient conditions. For the new testrig major improvements with respect to operation at high temperatures and high pressure have been made. The setup is illustrated in Fig. 1.

It allows high precision acoustic measurements of the damping performance of various liner configurations, including grazing and bias flow. A test signal is generated by either the upstream (A) or the downstream speaker (B) and is simultaneously measured by all microphones 1-10. It is ususally attenuated in the damping module by the interaction of the acoustic waves with the installed liner sample. By combining the measured signals upstream and downstream of the damping module, transmission, reflection, and dissipation can be determined (see section “EXPERIMENTAL ANALYSIS”). For measurements with grazing flow, two subsequent measurements are needed to fully characterize the liner sample.

The test duct consists of two symmetric measurement sections (section 1 and section 2 in Fig. 1) of 1670 mm length each. They have a circular cross-section with a diameter of 70 mm. In order to minimize the reflection of sound at the end of the duct back into the measuring section the test duct is equipped with anechoic terminations at both ends (not shown in Fig. 1).

A total of 10 microphone probes can be mounted to flanges within the upstream and downstream test sections. They are installed at different axial positions upstream and downstream of the damping module and are distributed exponentially with a higher density towards the damping module. A further microphone probe can be directly mounted to the damping module allowing a direct measurement of sound pressure in the liner plenum. At the axial position of microphone probe 3 and 8, there are five more flanges, respectively, equally distributed around the circumference of the duct. These are used for an in-situ calibration of the probes taking one of the probes as reference. The microphone probes themselves and a further method of calibration are described in more detail in section “INSTRUMENTATION”. At the end of each section a loudspeaker is mounted at the circumference of the duct (*A* and *B* in Fig. 1). They deliver the test signal for the damping measurements. The signal used here is a multi-tone sine signal. All tonal components of the signal are in the plane wave range. The signal has been calibrated in a way that the amplitude of each tonal component inside the duct is about 102 dB.
The microphones used in these measurements are 1/4” G.R.A.S. type 40BH condenser microphones, fitted in the pressure proof microphone probes. Their signals are recorded with a 16 track OROS OR36 data acquisition system with a sampling frequency of 8192 Hz. The source signals for the loudspeakers are recorded on the remaining tracks. The test signal is produced by an Agilent 33220A function generator. The signals are fed through a KME SPA 240E amplifier before they power the Monacor KU-516 speakers.

Two rotary screw compressors ESD-351 and ESD-301 provide compressed air as working fluid for the HAT facility. A maximum flow rate of 0.78 kg/s is available in sum for main flow, bias flow and the cooling flow of components (mainly microphone probes and loudspeakers). The pressure within the facility can be varied between nearly ambient (i.e. about 100 kPa) and 1100 kPa absolute pressure with a remote-controlled pressure valve. The mass flow rate can be varied by mounting throttles of different diameter (10-55 mm) to the downstream end of the facility. It is measured by a VARIOMASS eco meter upstream of the air heater. Several components are installed to obtain dry, oil- and condensate-free compressed air. With a custom-made electrical air heater system (maximum rating 500 kW) the working fluid can be heat up to 800 K before entering the actual test section. The secondary flow - namely bias flow for the damping module and the cooling flow for loudspeakers and microphone probes - are controlled independently from the main flow by various Bronkhorst mass flow controllers (ElFlow/InFlow) ranging from 1 to 400 kg/h. The available maximum pressure is about 1400 kPa.

Figure 2 shows a sketch of the relevant components of the test rig. Flanges between the different components yield good

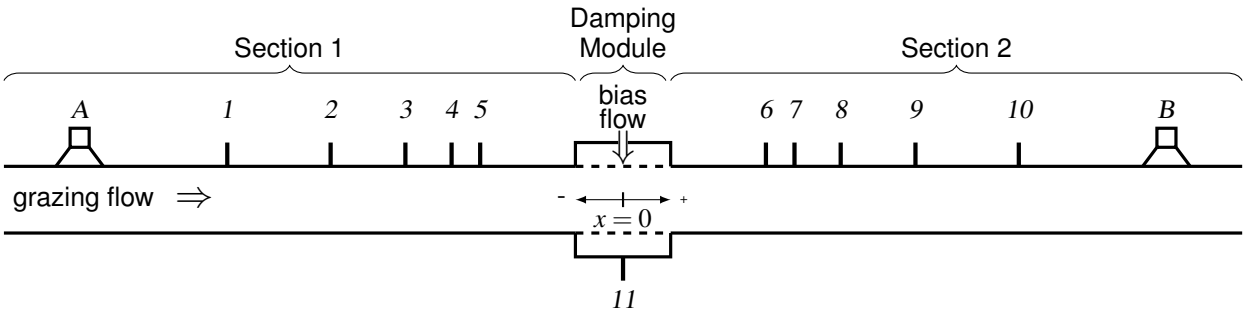

FIGURE 1: SCHEMATIC SETUP OF THE HOT ACOUSTIC TEST RIG (HAT) WITH SPEAKERS *A* AND *B*, AND MICROPHONES 1-10. THE ANECHOIC TERMINATIONS AT BOTH ENDS ARE NOT SHOWN.

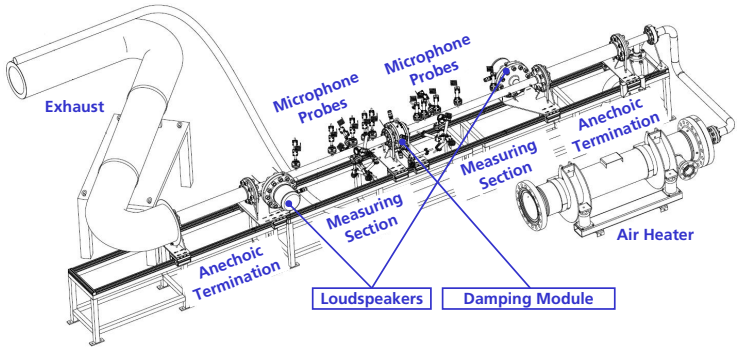

FIGURE 2: OVERVIEW OF THE COMPONENTS OF THE HOT-ACOUSTIC-TESTRIG (HAT).

accessibility for test installation and provide high flexibility for future upgrades.

INSTRUMENTATION

For the investigation of unsteady thermoacoustic phenomena, there is a need for high-accuracy unsteady instrumentation as well as for accurate assessment of the boundary and operating conditions.

Static Instrumentation

The mean temperature is measured at 9 positions via resistive thermal device (RTD's) of type Pt100 connected in four-wire configuration to a digital multimeter Agilent AG34972. In fact, the temperature is measured upstream and downstream of each loudspeaker and upstream and downstream of the liner sample. This enables the assessment of temperature gradients along the test section with the microphone probes and the quantification of the influcene of the cooling for loudspeakers and microphone probes. Further temperature sensors are located in the liner plenum measuring the actual temperature of the bias flow going through the liner module and in the loudspeaker module for health monitoring.

Static pressure is measured using pressure taps upstream and downstream of the liner and at three positions in the liner module. There, the taps are located at different radial positions which enables the accurate measurement of the pressure loss across the different bias flow liner samples which can be installed. The pressure drop across the throttling device is also determined. All pressure lines are fed into two fully differential Netscanner modules 9116 with separate sensors for absolute and differential pressure measurements (ranges: 2.5-1380 kPa).

Microphone Probes

For acoustic measurements in harsh environments, a dedicated microphone probe has been developed and used successfully for several years at DLR Berlin, e.g. for measurements at a laboratory combustion chamber. The proven design has recently undergone a major upgrade in order to cope also with pressurized environment up to 2000 kPa operating pressure. The new microphone probe is shown in Fig.3.

The new microphone probe - like the probe in its initial design - uses some standard G.R.A.S. 1/4" condenser microphone and pre-amplifier (type 40BH and 26AC), which are placed at a remote location for protection against heat and corrosive gases. The sound enters the probe from within the test facility through a tube which is mounted flush with the casing of the test facility. The microphone itself is placed perpendicular to the connection tube with its membrane flush to the tube wall. It is important to prevent reflections in this connection tube by extending it well beyond the location of the microphone membrane without a change in diameter - following the principle of a semi-infinite duct. The overall length of this tube is about one meter which is mostly wind up in spirals to save space. The large ratio between diameter and length of the connection tube provides sufficient damping of resonances over the frequency range of interest by viscous effects (see also Fig.5). A small amount of cooling air

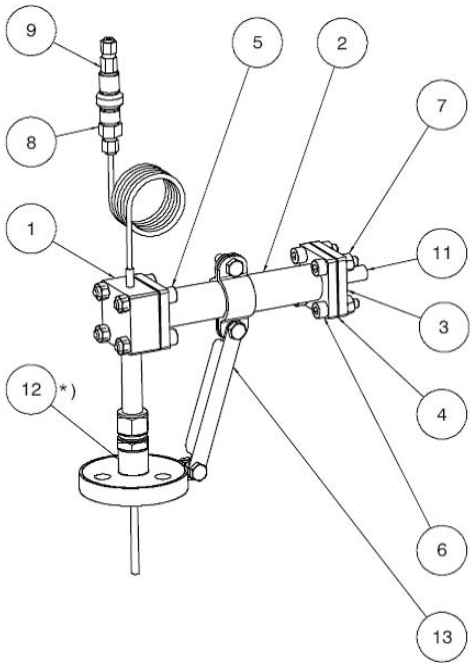

FIGURE 3: SKETCH OF THE NEW MICROPHONE PROBE USED FOR THERMOACOUSTIC INVESTIGATIONS

is fed through this tube preventing hot gases getting into contact with the microphone membrane. The supply tube of the cooling air supply further adds to the reduction of reflections by extending the virtual length of the probe tube, although the change in diameter certainly causes a - moderate - change in acoustic impedance.

With the microphone probes of the initial design, an investigation was made into the effect of cooling flow on the measurement results. It could be shown that under atmospheric conditions as little as 0.054 kg/h cooling air (which corresponds to a cooling flow velocity of 4 m/s) is enough to protect the delicate microphones. Detrimental noise components were found only for cooling flow velocities above 30 m/s. The required value for the cooling flow velocity holds also for applications with elevated pressure. However, the mass flow has to be adjusted according to the change in density of the cooling air.

The microphone probe will be mounted to the testrig via the large flange (no.12 in Fig.3) and sealed with a metal C-Ring. For thermal insulation, a fiber disc can be placed between upper and lower flange. The electrical connector (Lemo, no.11 in Fig.3) and the quick connector for the cooling air (Parker, no.8,9 in Fig.3) are rated beyond 2000 kPa. In case of a heavily vibrating testrig, a support beam (no.13) can be mounted yielding additional stiffness. However, this feature is not relevant for the application in the HAT facility with its steady operating characteristic. Sealing of the microphone protection tube (no.2) to the end pieces (no.1 and no.3) is accomplished by means of two graphite sealings.

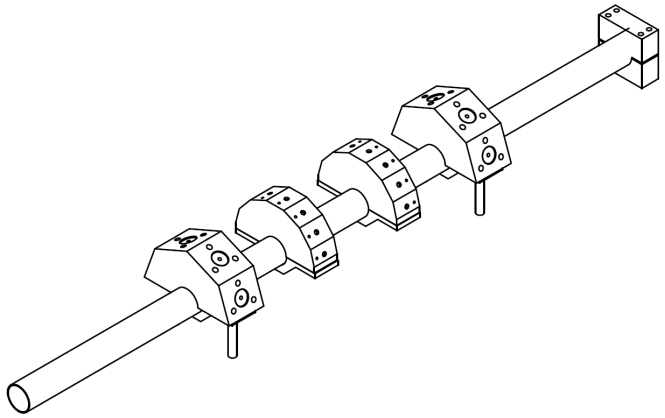

FIGURE 4: SKETCH OF THE CALIBRATION DUCT FOR MICROPHONE PROBES.

During testrig installation, the 6 mm tube protruding below the flange (no.12) is inserted in the respective counter flange that the tip of the tube is flush with the testrig casing wall. This ensures negligible disturbance for the flow field while exposing only the tip of the probe to the highest temperatures.

Due to the remote location of the microphone membrane compared to the sound field inside the test facility, a transfer function has to be determined via a calibration over the frequency range of interest (usually between 50 Hz and 4 kHz). Generally speaking, this transfer function is determined by the geometry of the probe, i.e. the thickness of the tube, the distance between the tip of the probe and the microphone membrane, and other dimensions of the microphone installation. It was aimed to keep volumina in front of the microphone as small as possible in order to avoid strong resonance at certain frequencies. Since this mechanical setup does not change once the probe is assembled, the transfer function does not change significantly over the period of time the probe is used. However, small variations in manufacturing and assembly require the determination of individual transfer functions for each probe. Prior to the determination of the transfer function and before each use, a quick one-point calibration with a pistonphone (250 Hz, 124 dB) is made. This provides an easy way for health checking of the microphone/pre-amplifier combination and by comparison with earlier readings spurious behaviour can be easily identified.

The transfer function can be determined in a specific calibration duct to which the microphone probes are attached. Figure 4 shows a sketch of this facility, where four microphone probes of the new design can be mounted at rings 1 and 4. A reference microphone can be directly attached at the bottom of each ring. The other two rings are used for microphone probes of the initial design. During the calibration, a loudspeaker is attached to the flange at the end of the tube.

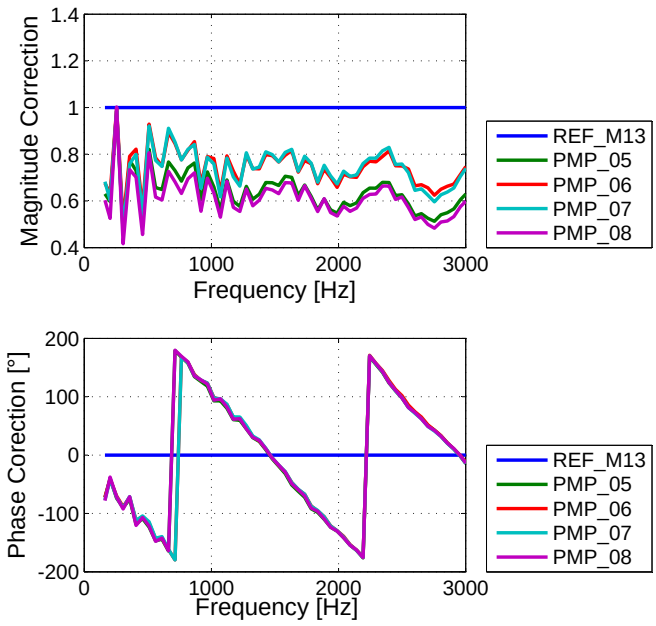

FIGURE 5: TRANSFER FUNCTION FOR MICROPHONE PROBES OBTAINED IN CALIBRATION DUCT.

The facility is operated at ambient conditions with the loudspeaker exciting plane waves over the frequency range of interest. By comparing the measured sound pressure level to the signal of the respective reference microphone which is directly attached to the duct, a correction for amplitude and phase is obtained (see example in Fig.5).

The magnitude of the pressure fluctuations at the excited frequency is divided by the magnitude measured by the reference microphone. A factor below unity indicates an attenuation of the signal through the remote location of the membrane in the microphone probe. For the phase correction, the difference between the phase of the probe microphone signal and the reference microphone signal is used. The increasing phase difference with increasing frequency resembles the decrease in wavelength while keeping the travel length (from tip to microphone membrane) constant. Therefore the phase jump at about 700 Hz and 2200 Hz is just an artefact from the ambiguity of the inverse trigonometric function which can be corrected by physical reasoning.

The four data sets in Fig.5 - belonging to four new microphone probes - show in general the same qualitative behaviour as could be expected due to their same dimensions. However, small deviations due to manufacturing tolerances cause the difference between the probes while the pairs (probe number 5 and 8, repectively 6 and 7) must be very similar.

The transfer funtion can be applied to acoustic measurements where the sound field is not known a-priori by correcting magnitude and phase of the spectral data in a postprocessing operation.

The second option of calibration - which is used for most of the investigations in the HAT facility - is to obtain a relative frequency calibration of the microphones by an in-situ calibration of the microphone probes. By installing all probes at the same axial location and exciting again acoustic plane waves, a relative calibration with respect to one microphone probe used as reference can be obtained. Since for the determination of reflection, transmission and dissipation coefficients only the ratio between the microphone signals is needed, the relative calibration is sufficient for most applications.

The microphon probes have been successfully tested in a combustion facility with respect to their safety up to 1350 kPa and 1500 K providing also at these conditions reproducable data of the high amplitude (up to 50 kPa) combustion noise.

Fast Thermocouple Probes

Although the determination of the mean temperature of the grazing and the bias flow is sufficient for the investigation of liners, for thermoacoustic experiments it is ususally of interest to determine also the fluctuations of the temperature with a high temporal resolution. Therefore, a specific thermocouple probes has been used in the past which consist of two very thin thermocouple sensors of different diameter. These are placed very close together in order to capture the temperature fluctuations at the same location (Fig. 6). The output signal of the thermocouple sensors follows a temperature change with a distinct time delay due to the phenomena of convection, radiation, conduction of heat. This low-pass behaviour of the sensors depends mainly on the size of the sensing elements. Thereby, a correction for these effects can be made in a post-processing operation. Dedicated experiments have shown the reliability of this method and a frequency resolution of at least 750 Hz. For the installation in the HAT facility, the double thermocouple probes have been equipped with a robust connection which can be mounted to the same flanges as the microphone probes are ususally mounted. If required a low-noise pre-amplifier can be directly incorporated in the probe improving the signal quality for long distances.

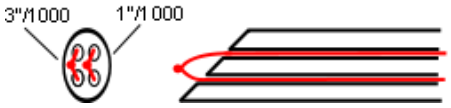

FIGURE 6: SKETCH OF THE PROBE HEAD OF THE DOUBLE THERMOCOUPLE PROBE.

EXPERIMENTAL ANALYSIS

For each configuration two different sound fields are excited consecutively in two separate measurements (index a and b). Speaker A is used in the first measurement and in the second measurement the same signal is fed into speaker B. Then, the data of section 1 and section 2 (index 1 and 2) are analyzed separately. This results in four equations for the complex sound pressure amplitudes for each section and measurement:

$$\hat{p}_{1a}(x) = \hat{p}^{+}_{1a} e^{-ik^{+}_{1}x} + \hat{p}^{-}_{1a} e^{ik^{-}_{1}x} \quad (1)$$

$$\hat{p}_{2a}(x) = \hat{p}^{+}_{2a} e^{-ik^{+}_{2}x} + \hat{p}^{-}_{2a} e^{ik^{-}_{2}x} \quad (2)$$

$$\hat{p}_{1b}(x) = \hat{p}^{+}_{1b} e^{-ik^{+}_{1}x} + \hat{p}^{-}_{1b} e^{ik^{-}_{1}x} \quad (3)$$

$$\hat{p}_{2b}(x) = \hat{p}^{+}_{2b} e^{-ik^{+}_{2}x} + \hat{p}^{-}_{2b} e^{ik^{-}_{2}x} \quad (4)$$

$\hat{p}^{+}$ and $\hat{p}^{-}$ are the complex amplitudes of the downstream and upstream traveling waves with their respective wave numbers $k^{\pm}$. The recorded microphone signals are transformed into the frequency domain using the method presented by Chung [3]. This method rejects uncorrelated noise, e.g. turbulent flow noise, from the coherent sound pressure signals. Therefore, the sound pressure spectrum of one microphone is determined by calculating the cross-spectral densities between three signals, where one signal serves as a phase reference. In our case the phase reference signal is the source signal of the active loudspeaker. As a result we obtain a phase-correlated complex sound pressure spectrum for each microphone signal.

According to Eqs. 1-4 the measured acoustic signal is a superposition of two plane waves traveling in opposite direction. In order to determine the downstream and upstream propagating portions of the wave in each section, a mathematical model is fitted to the acoustic microphone data. This model considers viscous and thermal conductivity losses at the duct wall. They are included in the wave number with the following attenuation factor α as proposed by Kirchhoff [4]:

$$\alpha = \frac{1}{cr}\sqrt{\frac{\eta\omega}{2\rho}}\left(1+\frac{\gamma-1}{\sqrt{Pr}}\right) \quad (5)$$

with the duct radius r, the speed of sound c, the dynamic viscosity η, the angular frequency ω, the density of the fluid ρ, the heat capacity ratio γ, and the Prandtl number Pr. As a result of this least-mean-square fit, the four complex sound pressure amplitudes $\hat{p}_1^{+}$, $\hat{p}_1^{-}$, $\hat{p}_2^{+}$ and $\hat{p}_2^{-}$ are identified at position x= 0 for both measurements. These sound pressure amplitudes are related to each other via the reflection and transmission coefficients of the test object. This is illustrated in Fig. 7 for the two different measurements *A* and *B*. In order to calculate the reflection and transmission coefficients r^{+}, r^{-}, t^{+}, and t^{-} from the sound pressure

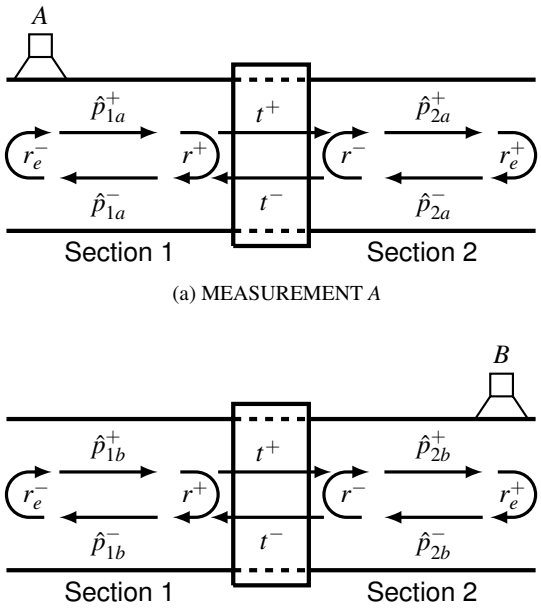

(a) MEASUREMENT *A*

(b) MEASUREMENT *B*

FIGURE 7: ILLUSTRATION OF THE SOUND FIELD IN THE DUCT FOR MEASUREMENTS *A* AND *B* BY MEANS OF THE SOUND PRESSURE AMPLITUDES $\hat{p}$, THE REFLECTION COEFFICIENT r, THE TRANSMISSION COEFFICIENT t, AND THE END REFLECTION r_e.

amplitudes the following four relations can be derived:

$$\hat{p}^{-}_{1a} = r^{+}\hat{p}^{+}_{1a} + t^{-}\hat{p}^{-}_{2a} \quad (6)$$

$$\hat{p}^{-}_{1b} = r^{+}\hat{p}^{+}_{1b} + t^{-}\hat{p}^{-}_{2b} \quad (7)$$

$$\hat{p}^{+}_{2a} = r^{-}\hat{p}^{-}_{2a} + t^{+}\hat{p}^{+}_{1a} \quad (8)$$

$$\hat{p}^{+}_{2b} = r^{-}\hat{p}^{-}_{2b} + t^{+}\hat{p}^{+}_{1b} \quad (9)$$

The equations from both measurements are combined and solved for the reflection

$$r^{+} = \frac{\hat{p}^{-}_{1a}\hat{p}^{-}_{2b} - \hat{p}^{-}_{1b}\hat{p}^{-}_{2a}}{\hat{p}^{+}_{1a}\hat{p}^{-}_{2b} - \hat{p}^{+}_{1b}\hat{p}^{-}_{2a}} \qquad r^{-} = \frac{\hat{p}^{+}_{2b}\hat{p}^{+}_{1a} - \hat{p}^{+}_{2a}\hat{p}^{+}_{1b}}{\hat{p}^{+}_{1a}\hat{p}^{-}_{2b} - \hat{p}^{+}_{1b}\hat{p}^{-}_{2a}} \quad (10)$$

and transmission coefficients

$$t^{+} = \frac{\hat{p}^{+}_{2a}\hat{p}^{-}_{2b} - \hat{p}^{+}_{2b}\hat{p}^{-}_{2a}}{\hat{p}^{+}_{1a}\hat{p}^{-}_{2b} - \hat{p}^{+}_{1b}\hat{p}^{-}_{2a}} \qquad t^{-} = \frac{\hat{p}^{+}_{1a}\hat{p}^{-}_{1b} - \hat{p}^{+}_{1b}\hat{p}^{-}_{1a}}{\hat{p}^{+}_{1a}\hat{p}^{-}_{2b} - \hat{p}^{+}_{1b}\hat{p}^{-}_{2a}} \quad (11)$$

in downstream and upstream direction, respectively. The advantage of combining the two measurements is that the resulting coefficients are independent from the reflection of sound at the duct

terminations. These end-reflections are contained in the sound pressure amplitudes, but do not need to be calculated explicitly.

The dissipation of acoustic energy is expressed by the dissipation coefficient. The dissipation coefficient can be calculated directly from the reflection and transmission coefficients via an energy balance:

$$R^{\pm} + T^{\pm} + \Delta^{\pm} = 1 \tag{12}$$

The energy of the incident wave is partly reflected, partly transmitted, and partly absorbed by the damping module. R and T are the power quantities of the reflection and transmission coefficients, while r and t have been the pressure quantities. Blokhintsev [5] defines the acoustic energy flux I in a moving medium (see as well in [6]):

$$I = \frac{1}{\rho c}(1+M)^2 \langle p^2 \rangle \tag{13}$$

where $\langle p \rangle$ is the time-averaged acoustic pressure, ρ is the density of the medium, c is the speed of sound, and M is the mean Mach number. Integrating over the duct cross-section area A and using the pressure amplitude yields a relation between the acoustic pressure p and acoustic power P quantities:

$$P^{\pm} = \frac{A}{2\rho c}(1 \pm M)^2 \left|\hat{p}^{\pm}\right|^2 \tag{14}$$

Then, the energy coefficients can be given relative to the pressure coefficients as:

$$R^{+} = \frac{P_1^{-}}{P_1^{+}} = \frac{(1-M_1)^2}{(1+M_1)^2} \cdot \left|r^{+}\right|^2 \tag{15}$$

$$R^{-} = \frac{P_2^{+}}{P_2^{-}} = \frac{(1+M_2)^2}{(1-M_2)^2} \cdot \left|r^{-}\right|^2 \tag{16}$$

$$T^{+} = \frac{P_2^{+}}{P_1^{+}} = \frac{A_2}{A_1}\frac{\rho_1 c_1}{\rho_2 c_2}\frac{(1+M_2)^2}{(1+M_1)^2} \cdot \left|t^{+}\right|^2 \tag{17}$$

$$T^{-} = \frac{P_1^{-}}{P_2^{-}} = \frac{A_1}{A_2}\frac{\rho_2 c_2}{\rho_1 c_1}\frac{(1-M_1)^2}{(1-M_2)^2} \cdot \left|t^{-}\right|^2 \tag{18}$$

where the indices 1 and 2 refer to section 1 and section 2 of the duct as illustrated in Fig. 7. With $A_1 = A_2$, $\rho_1 = \rho_2$, $c_1 = c_2$, $M_1 = M_2 = M$, and Eq. 12 follows the definition of the energy dissipation coefficient:

$$\Delta^{\pm} = 1 - \left(\frac{(1 \mp M)^2}{(1 \pm M)^2} \cdot \left|r^{\pm}\right|^2 + \left|t^{\pm}\right|^2\right) \tag{19}$$

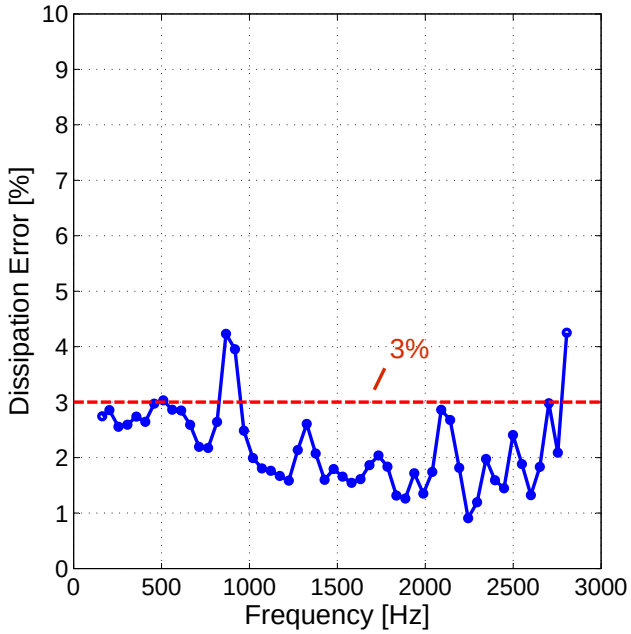

FIGURE 8: ERROR OF THE DISSIPATION COEFFICIENT IN THE EXPERIMENTAL RESULTS WITHOUT MEAN FLOW

This is an integral value of the acoustic energy that is absorbed while a sound wave is passing the damping module. The dissipation coefficient is used to evaluate the damping performance of the test object.

ACCURACY OF THE EXPERIMENTAL RESULTS

The test facility, the measurement techniques and the data analysis have been optimized to provide highest accuracy of the results. In order to provide a quantitative value for the accuracy a reference measurement with an unperforated reference sample installed in the damping module has been performed. For this configuration the dissipation coefficient is expected to be zero, i. e. no acoustic energy is absorbed. The deviation from this ideal value is the total error resulting from the uncertainties and systematic errors in the measurement chain and the subsequent analysis. The dissipation error is given as the deviation from the ideal value (zero) in percent. The downstream and upstream direction have been combined in an arithmetic averaged error of the dissipation coefficient:

$$\Delta_{err} = \frac{1}{2}\sqrt{(\Delta_{ref}^{+})^2 + (\Delta_{ref}^{-})^2} \tag{20}$$

A first measurement of the dissipation error was performed in the HAT without a mean flow being present. The dissipation

error is plotted over the frequency (Fig. 8). The dissipation error is mostly below 3 %, with values slightly above for frequencies around 800 Hz. As the frequency approaches the cut-on frequency (2870 Hz) of the first higher order mode ($kr = 1.84$) the error increases rapidly. This is due to the influence of evanescent modes which are becoming more prominent close to the cut-on frequency.
These results prove the high accuracy and the reliability of the experimental data. For the DUCT facility, the dissipation error is below 1 % for most of the frequencies below the cut-on frequency (data not shown here, see also [1]). However, this increase of the dissipation error is quite reasonable taking into account the much more complicated geometry of the microphone probes compared to microphones directly attached to the test section wall in the DUCT facility operating at ambient conditions.

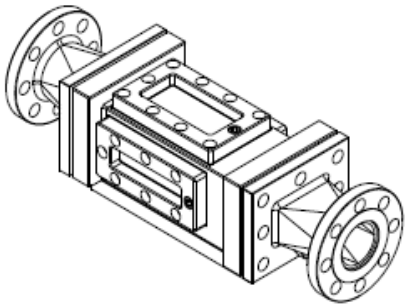

FIGURE 9: SKETCH OF THE PLANNED RECTANGULAR TEST SECTION REPLACING THE CURRENT DAMPING MODULE.

FUTURE PROJECTS AND UPGRADES

Since the actual commissioning of the HAT will take place in December 2010, here only a general description of the testrig, its main features and details of the measurement technique could be presented in this paper. However, some of the projects planned, upgrades that are already in the realization phase and some future options for the new facility shall be described in this section. Thereby, the opportunities for future research in this unique facility should become clear.

The primary field of interest is the investigation of bias flow liners under conditions relevant for aero-engine application, e.g. in the combustor region. By combining the results from the DUCT facility obtained at ambient conitions with the results of the HAT tests, effects due to elevated pressure and temperature will become visible. It will be possible to investigate also scaling rules by varying geometric dimensions (e.g. radius, perforated area etc.) which is of great practical interest for the application of liners.

Rectangular Test Section

One of the upgrades already planned and currently in the realization phase is a rectangular module which can be installed instead of the circular damping module of the initial configuration (Fig.9). It will include a three-side optical access enabling the use of optical measurement techniques (e.g. Laser Doppler Velocimetry, Particle Image Velocimetry) and increase the possibilities of test object installations. The primary point of interest is the investigation of blade rows e.g. with respect to the effectiveness of film cooling and overall assessment of aerodynamic performance which is one of the key areas of the universities' Chair of Aeroengines. For this type of investigations it is of great advantage, that the ratio between mean flow temperature and the temperature of the cooling fluid obtained in the HAT is nearly the same as in the turbine area of modern aeroengines. The rectangular module shall include also a boundary layer suction unit.

Beside the aerodynamic and aerothermal investigations, further aeroacoustic testing will be also possible with this module. Helmholtz liners which are currently being investigated in an rectangular setup of the DUCT facility can be installed in the new rectangular module. With the HAT facility it will be possible to analyze the performance of this liner samples for high grazing flow velocities with Mach numbers representative for aero-engine installation. The exploration of Helmholtz liners in high temperature environment is also of great interest due to the application of those liner types for the reduction of noise in the hot stream of APU units and on the splitter between core and bypass channel.

Zero-Mass-Flow Liner

An interesting improvement of the bias flow liners has been recently investigated in an explorative study in the DUCT facility. It could be shown by Heuwinkel et.al [7], that a broad band noise reduction could be also obtained with a perforated liner where the fluid in the plenum is excitet by a loudspeaker which subsequently generates small jets which in turn interact with the main flow and the acoustic field present in the duct (Fig.10).

In order to replace the loudspeaker and increase overall efficency of the setup, a dedicated noise generator without moving parts was designed which excites a high amplitude tone by a small amount of bias flow going through the plenum and the bias flow liner.

After the successful proof of concept and some parametric studies at ambient conditions, it is now of great interest to prove operation and optimize the setup under elevated pressure and temperature regimes which are typical for the application in the combustor of aero engines.

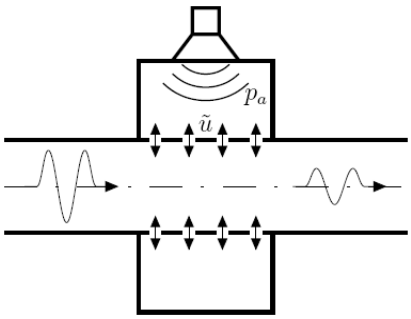

FIGURE 10: SKETCH OF THE WORKING PRINCIPLE OF A ZERO MASS FLOW LINER.

Indirect Combustion Noise

Through a series of dedicated experiments (see [8, 9]) it could be shown, that sound is generated when entropy or vorticity fluctuations are accelerated or decelerated. This phenomenon - called also indirect combustion noise - is presumably present in all aero engines e.g. due to the inhomogenous temperature and flow field exiting the combustor and entering the first turbine stage. However, a quantitative estimate of the contribution of indirect combustion noise compared to the overall core noise has not been obtained so far for aero engines. With the HAT facility the exploration of this phenomenon in a temperature-pressure range more representative for aero engines would be feasible. Therefore, some modification to the current setup would be needed (see Fig. 11).

This includes mainly a entropy or vortex generator module (e.g. injection of liquid nitrogen; the heated wires used in the original experiment would not yield a sufficient change in entropy) and a nozzle module in which the flow is subsequently accelerated up to a Mach number of unity. The instrumentation needed (i.e. microphone probes etc.) are already available in the current setup and could be used for these investigations.

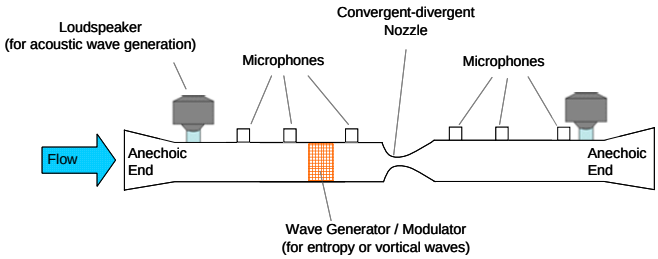

FIGURE 11: SCHEMATIC SETUP OF THE HAT IN A POSSIBLE CONFIGURATION FOR THE INVESTIGATION OF INDIRECT NOISE GENERATION.

Conclusions

The new Hot-Acoustic-Testrig which was erected in a cooperation between the German Aerospace Center (DLR) and the Berlin Institute of Technology, Chair of Aeroengines, has been described. The initial task after the commissioning will be the detailed investigation of aero-acoustic liners under conditions relevant to aero-engine applications. However, due to the effective modular construction of the facility a wide range of thermoacoustic experiments is envisaged for the future. Already planned experiments range from cooling effectiveness of turbine blades to the exploration of indirect combustion noise. The available instrumentation has been described in detail as was the data assessment to be applied to the liner investigations. The new facility already proved their design for high accuracy investigations by a reference measurement and will extend the experimental capabilites of the involved partners far beyond the current status.

ACKNOWLEDGMENT

The erection of the HAT facility was funded by the German Aerospace Center and the Institute of Technology Berlin, Chair of Aero Engines. The design of the microphone probes was funded within the EC-project TEENI. The financial support is gratefully acknowledged.

REFERENCES

[1] Heuwinkel, C., Sadig, S., Gerendás, M., Enghardt, L., and Bake, F., 2010. "Establishment of a high quality database for the modelling of perforated liners". In ASME Turbo Expo 2010, 14-18 June 2010, Glasgow, UK. GT2010-22329.

[2] Busse, S., Richter, C., Nitsch, S., Thiele, F., Bake, F., Enghardt, L., Kückens, C., and Müller, U., 2010. "Acoustic investigation of a specially manufactured non- locally reacting liner for aircraft application". In 16th AIAA/CEAS Aeroacoustics Conference, 7-9 June 2010, Stockholm, Sweden. AIAA-2010-3830.

[3] Chung, J., 1977. "Rejection of flow noise using a coherence function method". *Journal of the Acoustical Society of America,* ***62***(2), pp. 388–395.

[4] Kirchhoff, G., 1868. "über den Einfluss der Wärmeleitung in einem Gase auf die Schallbewegung". *Annalen der Physik und Chemie,* ***210***(6), pp. 177–193.

[5] Blokhintsev, D. I., 1946. *Acoustics of a nonhomogeneous moving medium.* NACA Technical Memorandum 1399 (1956). Originally published 1946 in russian language.

[6] Morfey, C. L., 1971. "Acoustic energy in non-uniform flows". *Journal of Sound and Vibration,* ***14***(2), pp. 159–170.

[7] Heuwinkel, C., Pardowitz, B., Bake, F., Röhle, I., and Enghardt, L., 2009. "On the excitation of a zero mass flow liner for acoustic damping". In 15th AIAA/CEAS Aeroa-

coustics Conference, 11-13 May 2009, Miami, FL. AIAA-2009-3110.

[8] Bake, F., Kings, N., Fischer, A., and Röhle, I., 2009. "Indirect combustion noise: Investigations of noise generated by the acceleration of flow inhomogeneities". *Acta Acustica united with Acustica,* ***95***(3), May/June, pp. 461–469.

[9] Bake, F., Richter, C., Mühlbauer, B., Kings, N., Röhle, I., Thiele, F., and Noll, B., 2009. "The entropy wave generator (EWG): A reference case on entropy noise". *Journal of Sound and Vibration,* ***326***(3–5), pp. 574–598. http://dx.doi.org/10.1016/j.jsv.2009.05.018.